

Residual immunity and seasonality of an epidemic

Siyu Chen*

High Meadows Environmental Institute
Princeton University, Princeton, NJ 08544
*corresponding author: siyu.chen@princeton.edu

and

David Sankoff

Department of Mathematics and Statistics
University of Ottawa
150 Louis Pasteur Pvt
Ottawa, Ontario, Canada K1N 6N5
sankoff@uottawa.ca

Abstract

We present a dynamical model of the onset and severity of cyclical epidemic disease taking account not only of seasonal boosts during the infectious season, but also of residual immunity remaining from one season to the next. After studying the mathematical properties of the model and the role of its parameters, we focus on the effect of titers remaining after one season on the timing and severity of the onset of the next season's epidemic. Suppressing the epidemic for one season, or witnessing a strong surge for one season, both have lasting effects for a number of successive seasons.

1 Introduction

Determining the onset of epidemic outbreak, whether of an emerging, newly recognized, virulent pathogen [1] or of a recurrent seasonal infection [2, 3, 4], is a vexing problem both for epidemiological research and for population health planning. This has been stressed for a variety of recurrent viral epidemics worldwide [5, 6, 7].

In a previous study [8] of the residual immunity remaining after each cycle, often annual, of a recurrent infectious disease, we modelled the yearly trajectory of antibody titre as a function solely of the waning process and the functional form, namely the temporal distribution of infections over an infectious season. With this minimal model, purely analytic closed-form solutions separating the effects of the few parameters involved were derived.

One result of simulating that model over 100 successive epidemic cycles, with the output of one cycle serving as the input of the next, was a strong result predicting residual titre as a function of shift of peak infection from one season to the next.

In the present paper, we investigate the other component of the reciprocal connection between titre and seasonality, namely the effect of titre remaining after one season on the timing and severity of the onset of the next season's epidemic.

Our model, which already incorporates a probabilistic determination of peak seasonality, is naturally adaptable to our goal through the linking of the peak probabilities to the pre-season titres. And the severity, or amplitude, which in our model is linearly predictive of post-season titres, can be linked in the same way to the pre-existing titres.

Epidemiological study focuses on the individuals in a population, whether they are susceptible to infection, exposed to the pathogen, symptomatic, hospitalized, in ICU, recovered or deceased. Populations are subdivided by age, sex, socioeconomic level and geographical location. Epidemic models calculate the number of individuals with different statuses and account for their movements from one compartment to another. Nevertheless, the population average titre of antibodies against the pathogen implicated in the epidemic should track the overall progression of the epidemic. A titre-based model can avoid the numerous parameters required in compartmental models.

The onset and severity of an epidemic are largely unpredictable. But there was widespread prediction that the lowering of antibody levels against influenza [9] and RSV [10] as a side-effect of non-pharmaceutical interventions during the covid-19 pandemic (masking, testing, lockdown, isolation,...) would lead to early onset and increased severity of epidemics of these diseases after the pandemic. And this prediction was validated in subsequent seasons.

Many other factors may enter into the timing of the induction of an infectious season, such as climate, demographic changes, antigenic shift in the pathogen, changes in transmission patterns [5], and others. Nevertheless low residual titre levels remain a likely driver of early onset time and severity.

2 The model

2.1 The infectious cycles

Our model contains a minimum of elements, namely a probability distribution representing the time course of the infectious period, including parameters for peak infections, severity and duration, as well as a waning parameter. In addition, the I -th season requires an input titre, associated with a reference time T_{I-1} , which we take as the end of the $I - 1$ -st infectious season.

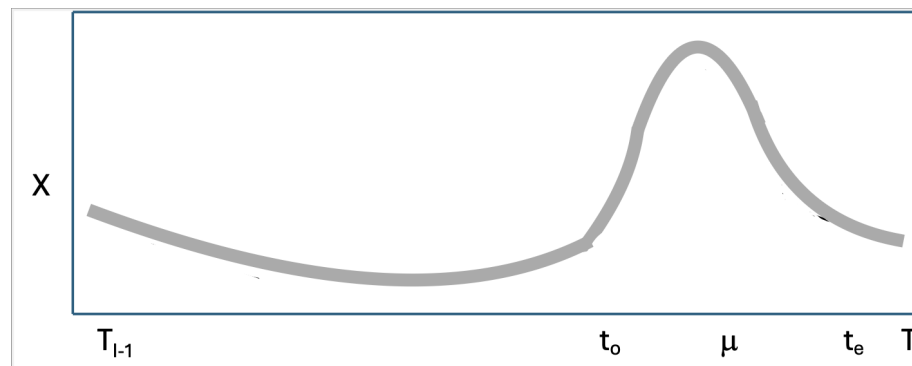


Figure 1: Concept of basic model.

As in Figure 1, the change of antibody titre between reference times T_{I-1} and T_I is represented by the equation:

$$X_{T_I} = X_{T_{I-1}} e^{-\omega(T_I - T_{I-1})} + \int_{T_{I-1}}^{T_I} A_I f_\mu(t) e^{-\omega(T_I - t)} dt, \quad (1)$$

where

- T_{I-1} is end of the previous cycle (in months),
- $X_{T_{I-1}}$ is the titre (in practice the log of the measured titre) at time T_{I-1} ,

- μ or μ_I is the peak month of the current infectious season,
- T_I is end of the current cycle,
- X_{T_I} is the titre (or log titre) at end of the current cycle
- ω is the decay parameter for exponential waning,
- A_I is the amplitude or severity of the infectious season,
- $f_\mu(t)$ is a probability density; our example this paper is based on a raised cosine, between onset date $t_o = \mu - \frac{\pi}{a}$ and end date $t_e = \mu + \frac{\pi}{a}$:

$$f_\mu = \frac{a}{2\pi}(1 + \cos a(t - \mu)) \quad (2)$$

for $t \in [t_o, t_e]$, and $f_\mu = 0$ elsewhere, with dispersion a^{-1} .

Equation (1) may be rewritten

$$X_{T_I} = X_{T_{I-1}} e^{-\omega(T_I - T_{I-1})} + A_I e^{-\omega T_I} \int_{t_o}^{t_e} f_\mu(t) e^{\omega t} dt. \quad (3)$$

The integral in this formula is

$$\int_{t_o}^{t_e} f_\mu(t) e^{\omega t} dt = e^{\mu\omega} \frac{\sinh(\pi\theta)}{\pi\theta(1 + \theta^2)}, \quad (4)$$

where $\theta = \frac{\omega}{a}$, so that Equation (1) becomes

$$X_{T_I} = X_{T_{I-1}} e^{-\omega(T_I - T_{I-1})} + A_I e^{-\omega(T_I - \mu)} \frac{\sinh(\pi\theta)}{\pi\theta(1 + \theta^2)}. \quad (5)$$

2.2 Studying a recurrent epidemic

Using initial titre input X_{T_0} to calculate X_{T_1} by Equations 1 or 5, and continuing the same way for X_{T_2}, X_{T_3}, \dots , we have defined a discrete dynamical system, at times $T_0 < T_1 < \dots$. We can assume $T_I - T_{I-1} > \Delta > 0$, for all $I \geq 1$. For two initial titres X_{T_0} and Y_{T_0} , we can see that

$$\|X_{T_n} - Y_{T_n}\| = \|X_{T_{n-1}} - Y_{T_{n-1}}\| e^{-\omega(T_n - T_{n-1})} \quad (6)$$

since the integral is constant, for $n = 1, 2, \dots$. Since $e^{-\omega\Delta} < 1$, this process is contractive, with Lipschitz constant $e^{-\omega\Delta}$. It has a fixed point

$$\frac{A_I e^{-\omega\delta} \frac{\sinh(\pi\theta)}{\pi\theta(1 + \theta^2)}}{1 - e^{-\omega\Delta}}, \quad (7)$$

in the simplest case, where $\delta = T_I - \mu$ and $\Delta = T_i - T_{i-1}$ for all I .

For example, we may examine the default parameters $A = 1, \omega = \frac{1}{24}, \mu = 12, a^{-1} = \frac{2}{\pi}, \Delta = T_I - T_{I-1} = 12, \delta = T_I - \mu = 3$, to determine the fixed point $X = 2.24$. This may be compared to the numerical results in Figure 2 tracking two trajectories of the model over 20 seasons.

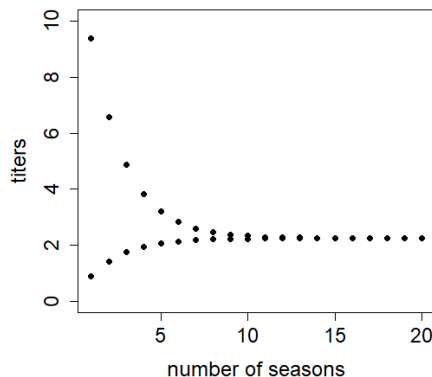


Figure 2: Convergence to fixed point from two initial points.

2.3 The role of the parameters

Waning, in limiting residual immunity in a seasonally recurring infectious disease, is an essential component of our model. Figure 3(a) shows the effect of this parameter. For very high waning rates, the output titre is decreased, while lower values of ω result in X_{T_I} conserving much of the input titre and even surpassing it.

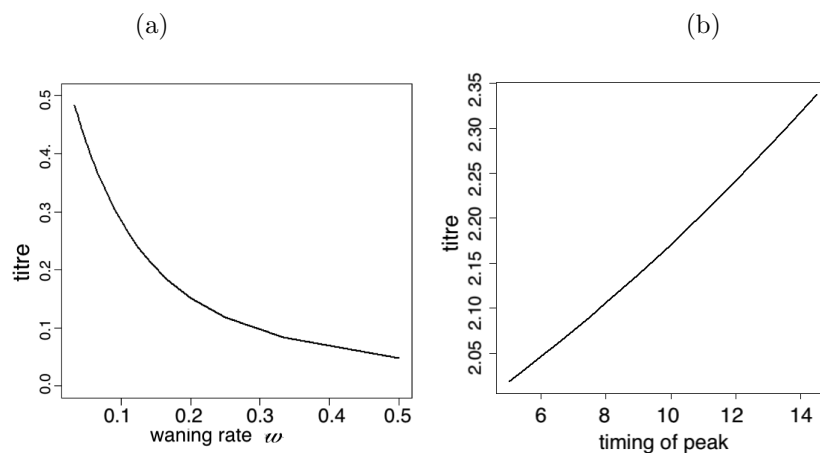


Figure 3: (a) Effect of the waning parameter ω on X_{T_I} . (b) Effects of early or delayed season.

As for the parameter representing seasonality, namely the peak infectivity date μ , an early or late season will increase or decrease the time until T_I , as seen in Figure 3(b), increasing or decreasing waning time, respectively. This

effect follows a largely linear response, and is substantial.

3 Long-term trends

3.1 Random peaks

As a benchmark experiment, we concatenated successive instances of the model of a single cycle described in Section 2 to carry out a simulation of 20 recurrent infectious seasons interspersed with quiescent periods for the rest of each cycle (i.e., year).

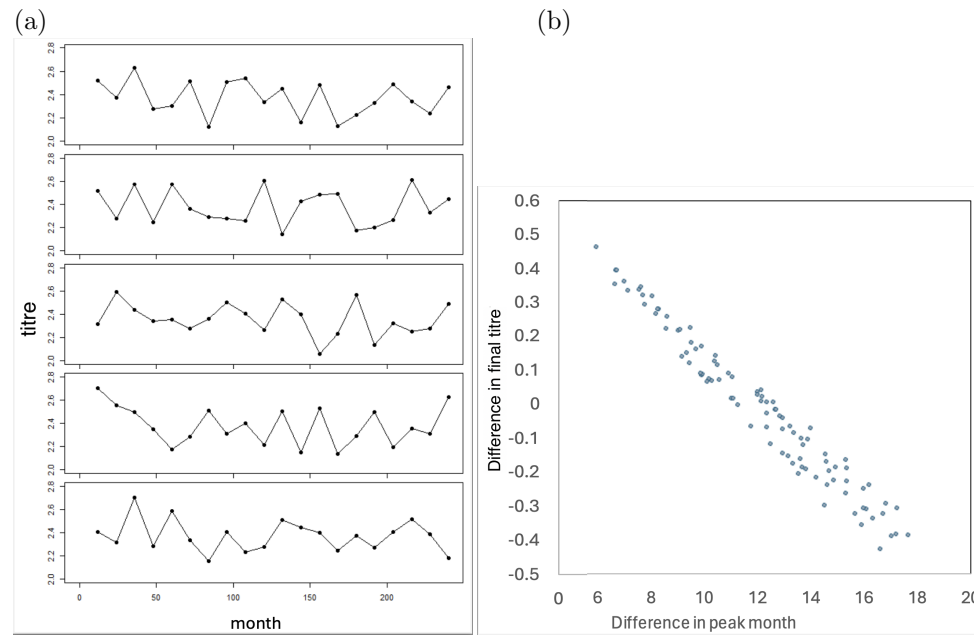


Figure 4: (a) Sample trajectories of 20 seasons produced by iterating the model, five replicates. (b) Association of titre change with length of inter-season times. From [1]

Initialized with a random titre at date T_1 corresponding to the end of a typical infectious period, the peak infection date m was chosen from a uniform probability over a wide range, September (month 9) to April (month 16), and the first iteration was performed with T_2 set to be $m + \frac{\pi}{a}$, with output X_{T_2} .

The output X_{T_2} at time T_2 from the first cycle, is then used as the starting titre X_{T_3} at time T_3 of the second cycle. The peak of infections is again randomly chosen from September to April.

This calculation is repeated for the third and subsequent cycles. Figure 4(a) shows five typical trajectories of X_T over the 20-year span. The randomness in the choice of peaks, and the small amount of noise added to the input every

year, meant that the process did not simply degenerate into a fixed point limit cycle, but maintained a stable pattern of random variation indefinitely.

We plotted the change in titre $\Delta_X = X_{T_I} - X_{T_{I-1}}$ as a function of $\Delta_\mu = \mu_I - \mu_{I-1}$, the shift in peak infections between the $I-1$ -st and I -th cycle. The results in Figure 4(b) show a tight linear relation between the two quantities. The slope is -0.9 titre units/12 months differential, or 0.075 units/month. This compares to $\log \omega = 0.042$ /month.

3.2 Training for seasonality

The negative correlation between the change of output titre and the time elapsed between successive peaks in Figure 4(b) must be seen as a function only of the waning time between two seasons, since there is no mechanism within the model to affect one year's peak μ as a direct function of the previous year's output titre $X_{T_{I-1}}$. Such a mechanism, however, is widely thought to be of importance to recurrent epidemics.

To train the model as a predictor of seasonality, we made use of the results of the experiment described in Section 3.1. Based on each year's X_{T_2} , a random choice of next year's peak month was effected. This choice involved two steps: The first was the deterministic choice of one of four bins, B_1, \dots, B_4 , with B_1 containing the highest values of X_{T_2} , and B_4 containing the lowest values of X_{T_2} . The second step was a uniform random choice among four consecutive months. The months in each bin overlapped those in the adjacent bins, with B_1 containing December through March, B_2 containing November through February, B_3 containing October through January and B_4 containing September through December.

A 200-season experiment could then be initiated by a random choice of X_{T_2} . Unlike the experiment in Section 3.1, there was no further addition of noise or other intervention over the length of the experiment. Because setting a new peak month determines a different fixed point for X_{T_2} , each iteration of the model gives an different output from the previous season's.

Figure 5(a) shows one aspect of the outcome, comparing the titres of each pair of successive seasons. The extent of the scatter is largely the effect of the large overlapping bins from which to choose the peak month.

3.3 Using the model to predict the peak of the next epidemic season

We regress the peak date chosen against the input titre for the data in Section 3.2. This produces the following result:

$$\text{peak month} = 2.815 \times \text{titre} - 0.068 + \epsilon \quad (8)$$

where the normal error ϵ has a standard deviation of 0.45 .

This result can then be used as a predictive tool. Given an end-of-season titre X_{T_2} , Equation (8) can predict the likely peak month and the shape of

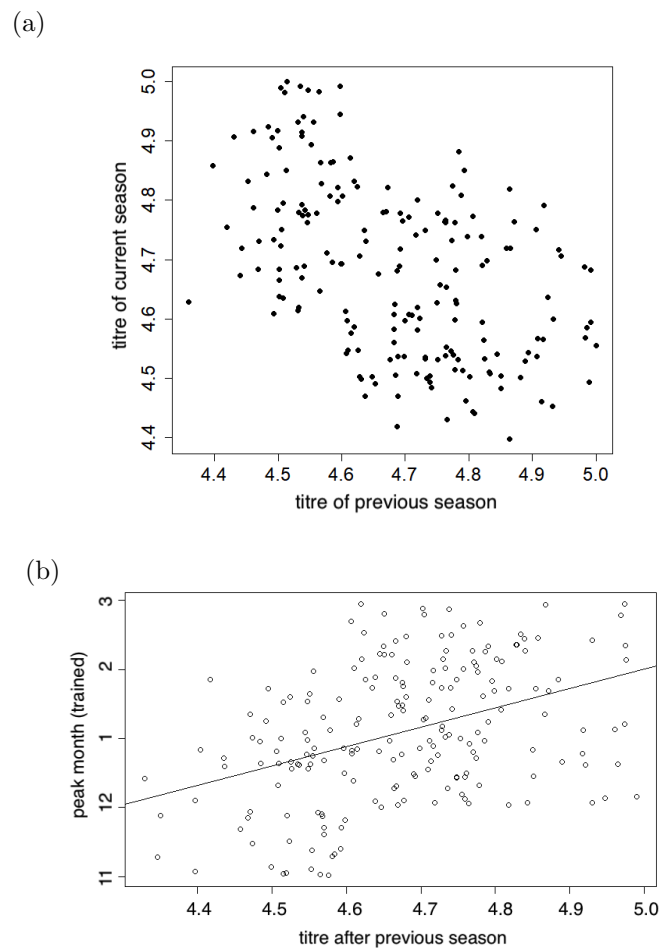


Figure 5: (a) Effect of training on titres of successive seasons. (b) Effect of training on choice of peak month, with regression line.

the titre distribution during the season. For example, using the parameters in Figure 5(b), an end-of-season titre of 4.7 predicts an early January peak, but distributed with a standard deviation of about two weeks.

3.4 Lasting effects of a missing season

The dramatically diminished influenza epidemic resulting from the covid pandemic-inspired non-pharmaceutical interventions in 2020-22 was followed by an early onset and severe influenza season in 2022-2023. This was predictable [9], given the lack of newly acquired immunity during the pandemic.

From the modeling viewpoint, this aspect of the seasonality-titre relationship, can be expressed by simply introducing a single missing (zero-amplitude)

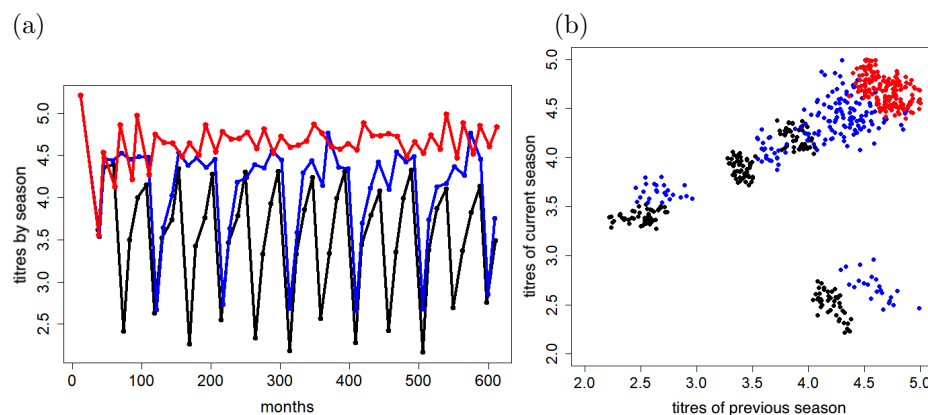


Figure 6: (a) End-of-season titre trajectories with an 8-year pattern of a missing season (blue), a 4-year pattern (black) and with no missing seasons. (red). (b) Change of titre from one season to the next. Displaced clusters represent the immediate effect of the missing boost.

season, and following the trajectory of the process in subsequent years.

To accomplish this we started with the model in Section 3.2. In one experiment over fifty years, we introduced an " $A = 0$ " year every eighth year. In a second experiment we introduced an " $A = 0$ " year every four years. We then compared the trajectory from these two experiments with that from the original, unmodified, experiment, where $A = 1$ for every season.

The results in Figure 6 show that for the experiment with an 8-year cycle, the effect of a reduced titre persisted over five to seven years, before catching up to the sequence of unmodified seasons. On the other hand, with a four-year cycle, the output titre never quite caught up .

Figure 6(a) summarizes the differences among these trajectories.

Figure 6(b) shows how the titres of the two missing-seasons trajectories gradually increase towards the unmodified (no missing seasons) pattern.

3.5 Lasting effects of a severe season

In a way analogous to the method in the Section 3.4, we can model the after-effects of a severe season, by setting $A = 2$ for one season out of four, or one season out of eight, while $A = 1$ for all the remaining seasons. The results of this experiment mirror those of the "missing season" experiment, but in the opposite direction. Figure 7 (a) shows how the titres in the 8-year pattern eventually settle down to rates comparable to the unmodified sequence, while the 4-year pattern retains elevated titres throughout.

Figure 7(b) shows how the titres of the two missing-seasons trajectories gradually decrease towards the unmodified (no severe seasons) pattern.

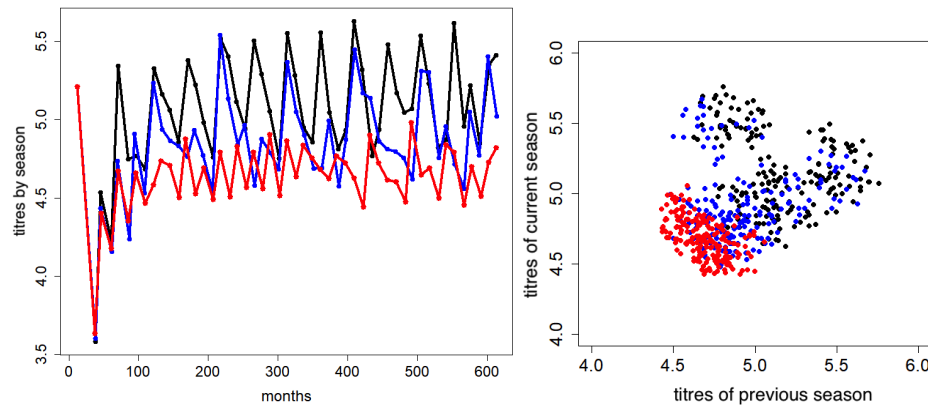


Figure 7: (a) End-of-season titre trajectories with an 8-year pattern of severe seasons (blue), a 4-year pattern (black) and with no severe seasons (red). (b) Change of titre from one season to the next. Displaced clusters represent the immediate effect of the amplified boost.

4 Discussion and conclusions

The core of our experimental model takes into account only titre increases during a few months-long season of an infectious disease with fixed infectivity peak μ , plus a continuous process of waning, expressed by a negative exponential with parameter ω . These two processes can reproduce the cycle of boosting and waning characteristic of recurrent seasonal infectious disease.

Iterating this model, however, is not suitable for generating long term trajectories of an epidemic. Mathematically, it is a contractive process that will quickly converge towards a sequence of identical seasons.

Replacing the assumption of fixed peak times with a random choice among several months, however, nullified the contractive tendency, so that we could explore the variation in titre as a function of the peak location parameter μ . This revealed a strong association between shift of peak month and change of titre at the end of the season.

Introducing an element of causality into this association, we trained the model so that a lower titre in the previous year would lead to an early onset in of the epidemic in the current year, via a slight bias in the random selection of the peak month, while a larger titre would delay the season.

The pattern that emerged from this training then allowed us to establish a prediction rule so that from the titre at the end of one season, we can predict the timing of the next one, in terms of a probability distribution of the timing of the peak month.

Inspired by the dramatic drop of infections by non-covid respiratory viruses like influenza and RSV in the 2021-2022 season, followed by a strong resurgence in the following year, we adapted our model by setting the amplitude (severity)

parameter A to zero for one year out of four or one year out of eight and observed how such perturbations affected subsequent years.

These experiments showed that after each of the “missing” years, the trajectories of the post-season titres inevitably recovered towards the usual pattern, largely in the case of the four-year cycle, but completely in the case of the eight-year cycle. This timing is of course dependent on our choice of parameters and protocols: ω , A , the training protocol, and predicting the distribution of μ . Nevertheless, it illustrates the kind of investigation possible with our titre-based modelling.

Our discussion has been phrased in terms of antibody titres, but the generality of our model means that it is not specifically limited to any specific aspect of the infectious disease season or yearly cycle, such as exposures, infections, symptoms, seroprevalence or antibody levels, as long as the annual boost can be represented by a distribution.

In this work, we have not assumed anything about viral strains. Apparent waning over several seasons may reflect mutational drift or selection in the antigen, rather than immunological processes per se. This does not distract from the pertinence of our model as a basis for analyzing the cyclical behaviour of boosting and waning.

References

- [1] Chen S, Flegg JA, White LJ, Aguas R. Levels of SARS-CoV-2 population exposure are considerably higher than suggested by seroprevalence surveys. *PLoS computational biology*. 2021 Sep 20;17(9):e1009436.
- [2] C.J. Rhodes, T.D. Hollingsworth, Variational data assimilation with epidemic models, *Journal of Theoretical Biology*, Volume 258, Issue 4, 2009.
- [3] Giorgia Vattiato, Audrey Lustig, Oliver J. Maclaren, Michael J. Plank, Modelling the dynamics of infection, waning of immunity and re-infection with the Omicron variant of SARS-CoV-2 in Aotearoa New Zealand, *Epidemics*, Volume 41, 2022, 100657.
- [4] Won M, Marques-Pita M, Louro C, Gonçalves-Sá J. Early and real-time detection of seasonal influenza onset. *PLoS computational biology*. 2017 Feb 3;13(2):e1005330.
- [5] Dalziel BD, Bjørnstad ON, van Panhuis WG, Burke DS, Metcalf CJ, Grenfell BT. Persistent chaos of measles epidemics in the prevaccination United States caused by a small change in seasonal transmission patterns. *PLoS computational biology*. 2016 Feb 4;12(2):e1004655.
- [6] Baker RE, Park SW, Yang W, Vecchi GA, Metcalf CJE, Grenfell BT. The impact of COVID-19 nonpharmaceutical interventions on the future dynamics of endemic infections. *Proc Natl Acad Sci USA* 2020; 117: 30547–53.

- [7] Messacar K, Baker RE, Park SW, Nguyen-Tran H, Cataldi JR, Grenfell B. Preparing for uncertainty: endemic paediatric viral illnesses after COVID-19 pandemic disruption. *The Lancet*. 2022 Nov 12;400(10364):1663-5.
- [8] Chen S, Sankoff D. A minimal model of boosting and waning in a recurrent seasonal epidemic. arXiv:2404.12865
- [9] Krauland MG, Galloway DD, Raviotta JM, Zimmerman RK, Roberts MS. Impact of Low Rates of Influenza on Next-Season Influenza Infections. *Am J Prev Med*. 62(4):503-510 (2002).
- [10] Hamid S, Winn A, Parikh R, et al. Seasonality of Respiratory Syncytial Virus — United States, 2017–2023. *MMWR Morb Mortal Wkly Rep* 2023;72:355–361.